JCTC Journal of Chemical Theory and Computation

Article

pubs.acs.org/JCTC

Ab Initio Molecular Dynamics Study of the Very Short O−H···O Hydrogen Bonds in the Condensed Phases

Piotr Durlak* and Zdzisław Latajka

Faculty of Chemistry, University of Wrocław, Joliot-Curie 14, 50-383 Wrocław, Poland

ABSTRACT: In this paper are presented the results of theoretical studies of the structure and proton motion in very short O···O intramolecular hydrogen bonds in two molecular crystals. A comparison was conducted between 3-cyano-2,4-pentanedione (**I**) and 4-cyano-2,2,6,6-tetramethyl-3,5-heptanedione (**II**) in the solid state. The dynamics of proton motion in the O−H···O hydrogen bond were investigated in he NVT ensemble at 298 and 50 K, respectively, for crystals **I** and **II** using Car−Parrinello and path integral molecular dynamics. Very large delocalization of the bridging proton was noted especially in the path integral simulation where quantum effects are taken into account. The infrared spectrum was calculated, and a comparative vibrational analysis was performed. CPMD vibrational results appear to be in qualitative agreement with the experimental ones.

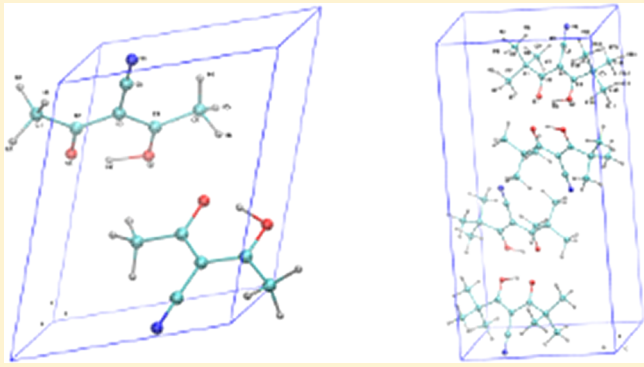

1. INTRODUCTION

Hydrogen bonds (HB) are ubiquitous in nature, so the concept of hydrogen bonding is of fundamental importance in many disciplines across physics, chemistry, and biology.[1] A vast number of publications on the structure and dynamics of different types of hydrogen bonds prove that researchers are becoming increasingly interested in this field of chemistry. Over the past several decades, much attention has been paid to the problems of proton transfer along H bonds in different molecular systems, for example in the gas phase,[2−4] H-bonded clusters in liquid water,[5−7] and in the condensed phase.[8,9] Nevertheless, there is still a lack of experimental and theoretical data in the literature on dynamics and proton transfer in very short hydrogen bonds in the crystalline systems. A detailed understanding of the structure and dynamics of short hydrogen bonding is a long-standing problem and continues to pose a significant challenge to experimental and computational investigations.[10,11]

In order to explain the appearance of strong and very strong intra- and intermolecular H bonds in some molecular systems, Gilli and co-workers introduced the concept of a resonance-assisted hydrogen bond (RAHB) where the H-bond donor and acceptor are connected through π-conjugated double bonds.[12−17] For example, for β-diketones and similar systems with a large O···O distance, a high degree of bond alternation (C−O and C═O bonds) was observed. However, with a shortening hydrogen bond distance, the distinctions between single and double bonds within this space are much smaller. Therefore, it has been suggested that hydrogen bond strength depends on the degree of resonance within the π-conjugated double bonds. It should be mentioned that, due to the consequences of π-electron delocalization, the intramolecular H bonds are characterized by a shortening of the O···O intermolecular bond length up to 2.4 Å, or less, a strengthening of the H bond, and the proton being shifted toward the center of the O···O bond.[17] In recent years, several review papers were published on the RAHB.[18−21] The most recent research concerning the existence of two tautomeric forms of β-diketones in the solid state was presented by Bertolasi and co-workers.[22] The authors stated that the number of β-keto−enol structures is far greater than the number of β-diketo ones, owing to the stabilization energy gained by the formation of the strong intramolecular O−H···O resonance-assisted hydrogen bonds. Moreover, in the intramolecular hydrogen bond, the tautomeric equilibrium O−H···O and O···H−O as well as the barrier height for proton motion may be strongly influenced by the substituent and to some degree by their crystal environments (for example see refs 22−24).

In addition to studies using malonaldehyde as a key case of RAHB[21,24] in recent years, other systems were studied extensively as well. In this largest group of molecules, the most examined are nitromalonamide,[23,25−27] 2-acetyl-1,8-dihydroxy-3,6-dimethylnapthlane,[28−31] and benzoylacetone.[32,33] In these papers, the properties of very short HBs have been characterized by extensive combined neutron and X-ray diffraction experiments, and they were also studied theoretically.

In this article, we examine the structure and proton motion in one of the shortest intramolecular hydrogen bonds yet reported in the literature.[34,35] Neutron diffraction data shows that lengths between O···O atoms in a hydrogen bond are, respectively, 2.465 Å and 2.394 Å for 3-cyano-2,4-pentanedione[34] and 4-cyano-2,2,6,6-tetramethyl-3,5-heptanedione.[35] Bertolasi and co-workers[22] classified both compounds as belonging to a class of β-diketo−enols with R_2 substituents linked by an sp^2 or sp carbon. In both

Received: July 11, 2012
Published: October 26, 2012

 © 2012 American Chemical Society

systems, R_2 = CN, but R_1 = R_3 are different substituents. According to these authors, the shorter O···O distance in 4-cyano-2,2,6,6-tetramethyl-3,5-heptanedione is caused by the greater steric compression exerted by *tert*-butyl groups with respect to the methyl one. Moreover, on the basis of very accurate ab initio calculations, the predicted barrier height for proton motion in the O···O bridge in 2,2,6,6-tetramethyl-3,5-heptanedione in the gas phase is very low and equal to 1.02 kcal/mol.[24] Therefore, one can expect large mobility of the bridged proton inthe O···O H bond.

In this work, the results of molecular dynamics simulations of hydrogen motion in the intramolecular O···O H bond of 3-cyano-2,4-pentanedione and 4-cyano-2,2,6,6-tetramethyl-3,5-heptanedione crystals are presented for the first time. The simulations have been performed using the Car−Parrinello molecular dynamics (CPMD)[36] and the path integral molecular dynamics (PIMD) method,[36,37] which takes into account the quantum nature of the proton, and as a consequence it enables the description of movement of the proton tunneling over the potential barrier thoroughly.

2. COMPUTATIONAL DETAILS

A series of full geometry and cell optimizations with the London-type empirical correction for dispersion interactions as proposed by Grimme,[38] together with vibrational harmonic frequency calculations, was undertaken to localize the key stationary points on the potential energy surface (PES) of the 3-cyano-2,4-pentanedione (**I**) and 4-cyano-2,2,6,6-tetra-methyl-3,5-heptanedione (**II**) in the solid state. For both crystals, the structural data were taken from the neutron diffraction studies of Silvernail and co-workers[34] and Belot and co-workers,[35] respectively. Calculations were performed using the CRYSTAL09 program,[39,40] utilizing the DFT method with the PBE functional[41] with two shrinking factors (5, 5) to generate a commensurate grid of k-points in the reciprocal space, following the Monkhorst−Pack method.[42] Calculations were carried out with the 6-31d1G (for carbon and nitrogen),[43] 6-31d1 (for oxygen),[43] and 3-1p1G (for hydrogen)[43] basis sets. Vibrational frequencys calculation in the CRYSTAL09 were performed at the Γ point.[39]

Molecular dynamics calculations were carried out using the CPMD program, version 3.13.2.[44] The initial molecular configuration for the 3-cyano-2,4-pentanedione and the 4-cyano-2,2,6,6-tetramethyl-3,5-heptanedione crystals optimized using the preconditioned conjugate gradient (PCG) method with Periodic Boundary Conditions (PBCs) was employed for the solid state calculations. In these cases, real space Ewald summation of electrostatic interactions was carried out taking into account eight cell replicas in each direction. We also generated the Monkhorst−Pack mesh (2,2,2) for calculated k-points in the reciprocal space in each direction. The crystal data from the neutron diffraction studies of Silvernail et al.[34] and Belot[35] and their co-workers were selected as starting points. The crystals were monoclinic 3-cyano-2,4-pentanedione ($P2_1$) with cell dimensions of a = 7.099, b = 5.534, c = 8.892 Å, $\alpha = \gamma = 90°$, and β = 112.305° with two formula units in the unit cell (Z = 2) and 4-cyano-2,2,6,6-tetramethyl-3,5-heptanedione ($P2_1/c$) with cell dimensions of a = 9.957, b = 20.405, c = 5.979 Å, $\alpha = \gamma = 90°$, and β = 91.303° with four formula units in the unit cell (Z = 4). Molecular dynamics and path integral simulations (NVT ensemble) were carried out at 298 and 50 K, respectively, with a time step of 3.0 au (0.072566 fs), coupled to a Nosé−Hoover chains thermostat[45] at a frequency of 3200 cm^{-1}. An electronic mass parameter of 400 au was employed. Electronic exchange and correlation have been modeled using the gradient-corrected functional of Perdew, Burke, and Ernzerhof (PBE).[41] Core electrons were treated using the norm-conserving atomic pseudopotentials (PP) of Troullier and Martins,[46] while valence electrons were represented in a plane-wave basis set truncated at an extended energy cutoff of 60 Ry. Following the initial equilibration period, data were accrued for a further 75 ps for crystal **I** and 36 ps for crystal **II** for Car−Parrinello, and for both crystals imaginary time (40 ps) for the path integral dynamics simulation was used, respectively, for 10 (PI10) Trotter replicas (polymer-beads) using the normal mode variable transformation. The data were visualized using the VMD[47] program, with the path integral data first processed using a script by Kohlmeyer to calculate the centroid position of each set of polymer beads.[48]

The vibrational spectrum was also calculated using the Fourier transformation of the dipole autocorrelation function obtained from the dipole trajectories generated by the CPMD simulation facilitated by the scripts of Forbert and Kohlmeyer.[49]

3. RESULTS AND DISCUSSION

The molecular geometry (in the unit cell) and atom labeling of 3-cyano-2,4 pentanedione and 4-cyano-2,2,6,6-tetramethyl-3,5-heptanedione crystals are shown in Figures 1 and 2,

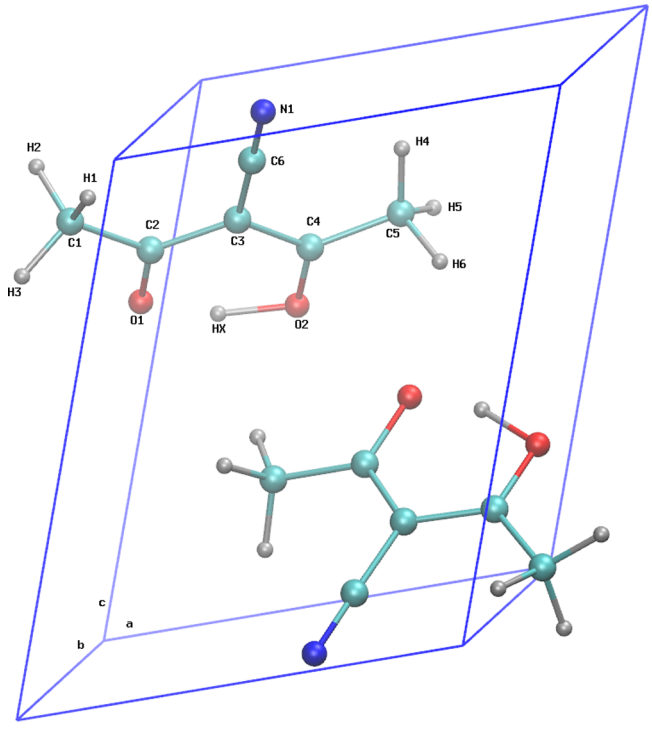

Figure 1. The unit cell and atom labeling of the 3-cyano-2,4-pentanedione crystal.

respectively. In Tables 1 and 2, calculated selected geometrical parameters after optimization compared with the average geometrical parameters from CPMD (standard deviation in brackets) and the existing experimental data for both crystals are presented. For crystal **I**, the distances between heavy atoms (O1−O2) in the hydrogen bond are very similar; however the average value coming from dynamics calculations is about 0.044 Å lower than experimental distance. The distance value between oxygen atoms coming from static calculations is most

dx.doi.org/10.1021/ct300589r | J. Chem. Theory Comput. 2013, 9, 65−72

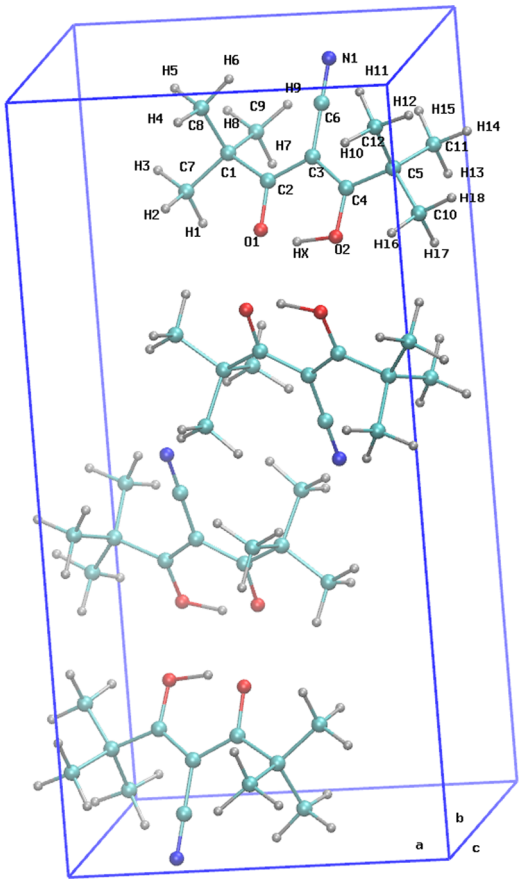

Figure 2. The unit cell and atom labeling of the 4-cyano-2,2,6,6-tetramethyl-3,5-heptanedione crystal.

similar to the experimental length; however the shortest length value for the hydrogen bond comes from the optimization on the PCG method level. The results from dynamics simulation and also geometry optimization indicate the slightly asymmetric position of the hydrogen (HX) atom between the two oxygen atoms, closer to the oxygen (O2). It is necessary to add that a hydrogen bond bridge is very nonlinear, and the angles oscillate within the range of 156−158°. The optimized parameters of the unit cell are in the very good accordance with the experimental values.[34] It seems to confirm the need to use dispersion corrections to the full energy for calculations on the DFT method level. For crystal **II**, distances between heavy atoms (O1−O2) in the hydrogen bond are also very similar; however the average value coming from dynamics calculations is about 0.017 Å lower than the experimental distance. In Table 2 it is shown that all methods of calculation, both the static optimization and CP dynamics simulation, showed a little lower of a length value between heavy atoms in HB against that of the experimental data.[34] In addition, we claim that the minimum value of the O1−O2 distances stems from the optimization on the DFT method level. Similarly, for crystal **II**, we observed a more symmetric position of the hydrogen (HX) atom between the two oxygen atoms.

The time evolution behavior of the bond lengths directly involved in the intramolecular hydrogen bonds from crystal **I** at 298 K and crystal **II** at 50 K are presented in Figure 3. The CP dynamic simulations were performed at two different temperature levels because the second crystal (4-cyano-2,2,6,6-tetramethyl-3,5-heptanedione) has a relatively low melting

Table 1. Calculated Selected Geometrical Parameters after Optimization Compared with the Average Geometrical Parameters from CPMD (Standard Deviation in Brackets) and the Existing Experimental Data for the 3-Cyano-2,4-pentanedione Crystal (Bond Lengths and Unit Cell Parameters Are in Å, Angles in deg)

parameter	PBE/6-31d1G/ 6-31d1/3-1p1G	PCG/60 Ry	CPMD/60 Ry/ 298 K/avg.	exptl.[34]
O1−O2	2.443	2.390	2.421 (0.059)	2.465
O2−HX	1.072	1.196	1.221 (0.127)	1.134
HX−O1	1.413	1.235	1.252 (0.132)	1.454
O1−C2	1.274	1.297	1.296 (0.127)	1.268
O2−C4	1.314	1.301	1.303 (0.027)	1.294
C3−C4	1.418	1.426	1.431 (0.321)	1.401
C3−C2	1.451	1.426	1.439 (0.034)	1.431
C3−C6	1.418	1.413	1.414 (0.027)	1.437
C6−N1	1.179	1.171	1.176 (0.017)	1.133
C2−C1	1.495	1.485	1.485 (0.031)	
C4−C5	1.484	1.470	1.489 (0.032)	
C1−H1	1.098	1.101	1.107 (0.031)	
C1−H2	1.103	1.102	1.108 (0.031)	
C1−H3	1.100	1.108	1.104 (0.031)	
C5−H4	1.102	1.103	1.105 (0.031)	
C5−H5	1.102	1.104	1.105 (0.030)	
C5−H6	1.096	1.105	1.104 (0.030)	
∠O1−HX−O2	156.20	158.78	156.24 (5.13)	
∠HX−O2−C4	104.24	101.43	102.21 (3.40)	107.42
∠O1−C2−C3	119.09	118.26	119.22 (2.59)	119.62
∠O1−C2−C1	120.00	118.86	118.52 (3.29)	118.72
∠C2−C3−C4	119.79	119.00	118.59 (2.39)	120.62
∠O2−C4−C3	118.82	119.46	119.26 (2.60)	119.82
∠O2−C4−C5	117.83	117.70	118.88 (3.29)	116.62
∠C4−C3−C6	119.48	119.79	119.94 (3.24)	119.82
∠C2−C3−C6	120.71	121.15	120.85 (3.21)	119.52
∠C3−C6−N1	179.72	179.07	172.77 (3.76)	179.72
∠C3−C2−C1	120.89	122.82	121.94 (3.39)	121.62
∠C3−C4−C5	123.34	122.84	121.50 (3.34)	123.42
∠C2−C1−H1	111.23	111.08	109.89 (4.60)	
∠C2−C1−H2	109.68	110.55	110.68 (4.88)	
∠C2−C1−H3	110.24	110.06	110.76 (4.93)	
∠C4−C5−H4	110.75	112.45	110.17 (4.75)	
∠C4−C5−H5	110.48	109.06	109.79 (4.75)	
∠C4−C5−H6	110.69	109.45	110.20 (4.77)	
a	6.937			7.099
b	5.538			5.534
c	8.351			8.892
α	90.00			90.00
β	114.27			112.30
γ	90.00			90.00

point. Careful analysis of the strong (O2−HX···O1) intramolecular hydrogen bond shows a very large fluctuation of the bridging proton between the two oxygen atoms in crystal **I** (see Figure 3a), and lesser mobility of the proton delocalizes in the hydrogen bridge of the second crystal (see Figure 3b) on account of the temperature of the simulation, which is also essential. The O2−HX bond length changes in the ranges of 0.9−1.59 Å for crystal **I** and 1.05−1.37 Å for crystal **II**.

Large delocalization of the bridging proton, especially in strong O2−HX···O1 hydrogen bonds from both crystals, is even more visible in Figure 4, where the comparison of the proton distribution in both O2−HX···O1 hydrogen bonds

dx.doi.org/10.1021/ct300589r | J. Chem. Theory Comput. 2013, 9, 65−72

Table 2. Calculated Selected Geometrical Parameters after Optimization Compared with the Average Geometrical Parameters from CPMD (Standard Deviation in Brackets) and the Existing Experimental Data for the 4-Cyano-2,2,6,6-tetramethyl-3,5-heptanedione Crystal (Bond Lengths and Unit Cell Parameters Are in Å, Angles in deg)

parameter	PBE/6-31d1G/ 6-31d1/3-1p1G	PCG/60 Ry	CPMD/60 Ry/ 50 K/avg.	exptl.[35]
O1−O2	2.368	2.376	2.377 (0.017)	2.394
O2−HX	1.162	1.203	1.203 (0.035)	
HX−O1	1.248	1.213	1.251 (0.037)	
O1−C2	1.283	1.293	1.293 (0.010)	1.274
O2−C4	1.293	1.295	1.295 (0.010)	1.273
C3−C4	1.439	1.438	1.439 (0.013)	1.429
C3−C2	1.451	1.441	1.442 (0.013)	1.432
C3−C6	1.418	1.412	1.413 (0.011)	1.432
C6−N1	1.181	1.175	1.175 (0.006)	1.149
C2−C1	1.523	1.527	1.530 (0.015)	1.526
C4−C5	1.522	1.525	1.525 (0.014)	1.523
C1−C7	1.538	1.537	1.539 (0.014)	1.536
C1−C8	1.548	1.541	1.543 (0.014)	1.540
C1−C9	1.547	1.547	1.548 (0.015)	1.534
C5−C10	1.538	1.540	1.541 (0.014)	1.539
C5−C11	1.544	1.548	1.550 (0.015)	1.529
C5−C12	1.547	1.540	1.541 (0.014)	1.546
C7−H1	1.101	1.101	1.102 (0.013)	
C7−H2	1.102	1.101	1.101 (0.012)	
C7−H3	1.100	1.102	1.102 (0.012)	
C8−H4	1.102	1.103	1.104 (0.012)	
C8−H5	1.103	1.107	1.108 (0.013)	
C8−H6	1.099	1.109	1.102 (0.013)	
C9−H7	1.101	1.104	1.103 (0.012)	
C9−H8	1.103	1.099	1.099 (0.012)	
C9−H9	1.098	1.103	1.105 (0.013)	
C10−H16	1.100	1.102	1.102 (0.012)	
C10−H17	1.102	1.101	1.103 (0.013)	
C10−H18	1.102	1.103	1.103 (0.013)	
C11−H13	1.097	1.101	1.102 (0.013)	
C11−H14	1.102	1.104	1.105 (0.012)	
C11−H15	1.102	1.101	1.100 (0.012)	
C12−H16	1.100	1.102	1.101 (0.012)	
C12−H17	1.103	1.101	1.102 (0.013)	
C12−H18	1.102	1.105	1.104 (0.012)	
∠O1−HX−O2	158.16	158.98	158.67 (1.92)	
∠HX−O2−C4	103.62	102.75	102.74 (1.32)	
∠O1−C2−C3	118.12	118.21	118.16 (0.99)	
∠O1−C2−C1	117.79	116.49	116.47 (1.16)	
∠C2−C3−C4	118.40	118.84	118.78 (0.93)	
∠O2−C4−C3	118.36	118.36	118.40 (1.02)	
∠O2−C4−C5	116.93	116.30	116.38 (1.16)	
∠C4−C3−C6	120.74	120.69	120.65 (1.21)	
∠C2−C3−C6	120.83	120.42	120.44 (1.22)	
∠C3−C6−N1	179.27	179.80	177.17 (1.45)	
∠C3−C2−C1	124.09	125.28	125.31 (1.21)	
∠C3−C4−C5	124.67	125.31	125.13 (1.19)	
∠C2−C1−C7	110.40	109.78	109.79 (1.25)	
∠C2−C1−C8	109.42	108.79	108.35 (1.46)	
∠C2−C1−C9	109.93	111.44	111.68 (1.48)	
∠C4−C5−C10	110.15	109.58	109.95 (1.20)	
∠C4−C5−C11	108.07	109.18	108.24 (1.60)	
∠C4−C5−C12	111.37	110.69	110.88 (1.55)	
∠C1−C7−H1	111.76	111.68	111.76 (1.76)	
∠C1−C7−H2	111.22	111.75	111.59 (1.76)	
∠C1−C7−H3	107.73	108.09	108.16 (1.76)	
∠C1−C8−H4	113.32	110.87	111.56 (1.78)	
∠C1−C8−H5	107.22	108.48	107.92 (1.77)	
∠C1−C8−H6	110.45	112.85	112.74 (1.83)	
∠C1−C9−H7	110.13	111.59	108.56 (1.81)	
∠C1−C9−H8	110.13	112.65	112.77 (1.82)	
∠C1−C9−H9	108.04	107.98	110.86 (1.78)	
∠C5−C10−H16	110.77	111.37	112.01 (1.77)	
∠C5−C10−H17	111.61	112.01	111.39 (1.81)	
∠C5−C10−H18	108.31	108.46	108.36 (1.76)	
∠C5−C11−H13	113.21	111.36	111.08 (1.82)	
∠C5−C11−H14	108.35	108.65	108.11 (1.80)	
∠C5−C11−H15	109.92	112.01	113.44 (1.83)	
∠C5−C12−H10	113.45	108.07	108.81 (1.84)	
∠C5−C12−H11	107.18	113.32	112.07 (1.83)	
∠C5−C12−H12	110.64	111.17	111.06 (1.88)	
a	9.695			9.957
b	20.084			20.405
c	5.694			5.979
α	90.00			90.00
β	88.36			91.30
γ	90.00			90.00

along the reaction coordinate from the CPMD and PIMD methods is presented. The reaction coordinate (δ parameter) is defined as the difference between O1−HX and HX−O2 bond lengths for the intramolecular H bond. The midpoint position of proton in the hydrogen bridge is described by reaction coordinate equal to zero. Careful analysis of the distribution function of the proton in the hydrogen bridge shows the importance of quantum effects at lower temperatures. As is visible in Figure 4b, the distribution function calculated at 50 K from PIMD simulations is very broad in comparison to the plot received from CPMD simulations. On the other hand, both plots of distribution functions presented in Figure 4a, which correspond to the simulations at 298 K, are almost identical.

Wilson and co-workers[50] conducted single neutron diffraction studies about the relation between the occupancy ratio parameter of the proton position and the temperature in the benzoic acid crystal. In this paper, the CPMD and PIMD calculated proton distribution functions of 3-cyano-2,4-pentanedione and 4-cyano-2,2,6,6-tetramethyl-3,5-heptanedione crystals were used to determine the occupancy ratio of the proton of the first crystal of 0.55/0.45 (CPMD) and 0.53/0.47 (PIMD) and for the second crystal of 0.50/0.50 (CPMD) and 0.52/0.48 (PIMD). Both values are in good agreement with the experimental data from neutron diffraction.[34,35] The hydrogen bond in crystal **II** is much more symmetrical than that in the first crystal. However, our results also confirm that structures **I** and **II** are slightly asymmetrical and the crystal structure forces the β-keto−enol form to appear more frequently, as was suggested by Bertolasi and co-workers.[22] We stated that the influence of the crystal structure caused a slight disturbance of the symmetry of the hydrogen bond in spite of the existing enol−enol tautomeric equilibrium.

Figure 5 shows the free energy profiles for proton motion obtained from CPMD and PIMD results. Free energy profiles were calculated following the equation

dx.doi.org/10.1021/ct300589r | J. Chem. Theory Comput. 2013, 9, 65−72

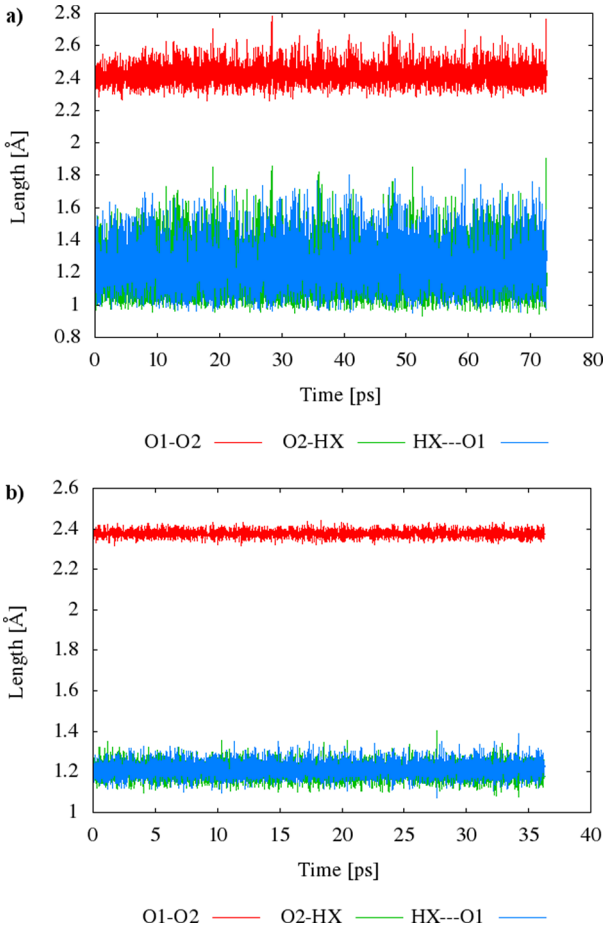

Figure 3. Time evolutions of bonds involved in the hydrogen bonds O2-HX···O1 (a) for 3-cyano-2,4-pentanedione at 298 K and (b) for 4-cyano-2,2,6,6-tetramethyl-3,5-heptanedione at 50 K from the CPMD calculations.

$$\Delta F = -kT \ln[P(\delta)] \quad (1)$$

where k is the Boltzmann constant, T is the simulation temperature, and $P(\delta)$ is the proton distribution as a function of δ (the reaction coordinate). This parameter gives a measure of the degree of proton transfer within the hydrogen bond, with a value of zero indicating the midpoint of the hydrogen bridge. The profiles of the free energy in Figure 5 demonstrate the absence of an effective barrier for proton transfer even without the inclusion of quantum effects for the CPMD simulation. The quantum effects taken into account do not change the effective potential shape drastically. We observed one minimum potential shape in each case, but for crystal **II** the profile of free energy obtained from CPMD is sharper than the profile energy from PI simulation (see Figure 5). It is important to add also that curves of the free energy for the 3-cyano-2,4-pentanedione crystal are slightly asymmetrical.

The extent of delocalization inside the resonant spacer can be estimated using the π-delocalization index, $\lambda = 1/2(1 - Q/0.32)$, introduced by Gilli et al.,[17] where for the system 3-cyano-2,4-pentanedione, $Q = (r_{C4O2} - r_{C2O1}) + (r_{C2C3} - r_{C3C4})$ and 4-cyano-2,2,6,6-tetramethyl-3,5-heptanedione $Q = (r_{C4O2} - r_{C2O1}) + (r_{C2C3} - r_{C3C4})$. It should be noted that a λ value of 0.5 indicates a fully delocalized keto−enolic system, whereas a λ value close to 0 or 1 indicate localized bonding. For calculations

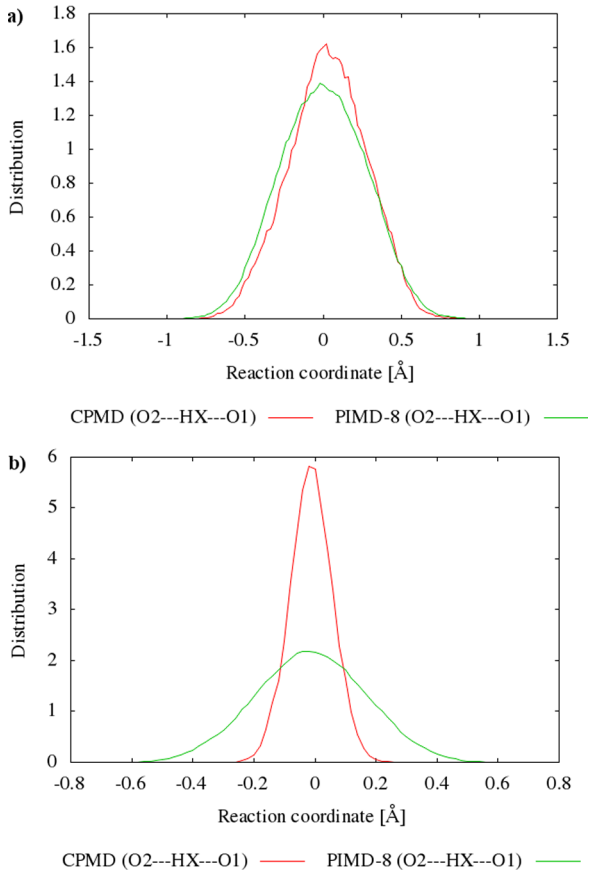

Figure 4. Comparison of the distribution functions (δ parameter) from CPMD and PIMD-8 for the intramolecular H bonds (a) for 3-cyano-2,4-pentanedione at 298 K and (b) for 4-cyano-2,2,6,6-tetramethyl-3,5-heptanedione at 50 K.

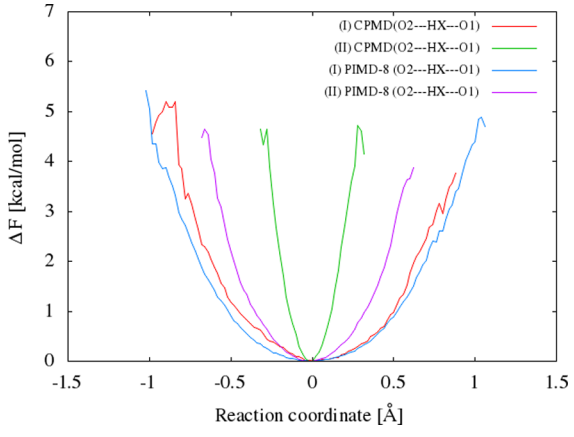

Figure 5. Comparison of the single proton transfers free energy ΔF profiles in crystalline 3-cyano-2,4-pentanedione (I) and 4-cyano-2,2,6,6-tetramethyl-3,5-heptanedione (II) from CPMD and PIMD-8 simulations for the intramolecular H bonds.

of the λ index, we have applied average values if bond distances are from the CPMD simulations. The π-delocalization index is equal 0.48 for **I** and 0.49 for **II**. It is worth mentioning that the analogous value for **II** was received on the basis of very accurate ab initio calculations in the gas phase.[24] On this basis, one can suggest the RAHB character of the hydrogen bond in studied systems.

dx.doi.org/10.1021/ct300589r | J. Chem. Theory Comput. 2013, 9, 65−72

Table 3. Calculated and Experimental Selected Vibrational Frequencies in (cm^{-1}) for the 3-Cyano-2,4-pentanedione in the Solid State

frequency	PBE/6-31d1G/6-31d1/ 3-1p1G harmonic/anharmonic	CPMD/ PBE/ 60 Ry	exptl.[34]
υ CH_3 assym.	3122	2990	2976
υ CH_3 symm.	3082	2950	2938
υ CH_3 symm.	2996	2885	2875
υ C═N	2232	2180	2217
υ OH	2151/1823	2150	
δ OH + υ C═O	1625	1570	1576
ρ CH_2	1335	1270	1210
υ C−O	1264	1180	1136
ρ OH	1180	1070	1029
δ CH_3	990	970	941
δ C═H	984	930	894
	676	670	637
	587	562	522
υ O−H−O	270	285	

Table 4. Calculated and Experimental Selected Vibrational Frequencies (in cm^{-1}) for the 4-Cyano-2,2,6,6-tetramethyl-3,5-Heptanedione in the Solid State

frequency	PBE/6-31d1G/6-31d1/ 3-1p1G harmonic/anharmonic	CPMD/ PBE/ 60 Ry	exptl.[34]
υ CH_3 assym.	3120	2960	3002
υ CH_3 assym.	3062	2920	2976
υ CH_3 symm.	2985	2860	2939
υ CH_3 symm.	2975	2840	2876
υ C═N	2216	2120	2211
υ OH	2140/1825	2100	
δ OH + υ C═O	1596	1650	1526
υ OH + υ C═O	1577	1530	1469
δ CH_2	1470	1429	1415
υ C−C + δ CH_2	1413	1400	1370
CH_3	1371	1357	1303
υ C−C + δ OH	1263	1258	1220
ρ OH	1176	1080	1082
ω CH_3	1026	1050	1028
δ CH_3	957	940	939
ρ CH_2	928	907	909
	918	890	872
	837	810	784
	779	760	732
υ O−H−O	223	210	

Vibrational analysis is very important since it proves that the results of molecular dynamics simulations are correct. The infrared spectrum is very sensitive to structural changes during simulation, especially for molecular systems with hydrogen bonds.[51] The vibrational spectra for 4-cyano-2,4-pentanedione and 4-cyano-2,2,6,6-tetramethyl-3,5-heptanedione in the solid state have been calculated using Fourier transformation of the dipole autocorrelation function obtained for dipole trajectories generated by CPMD simulation. It is important to point out that this approach includes anharmonic effects in all of the vibrational modes and takes into account the crystal effect. Selected characteristics of vibrational frequencies from the CPMD simulations, together with harmonic and anharmonic (only for −OH

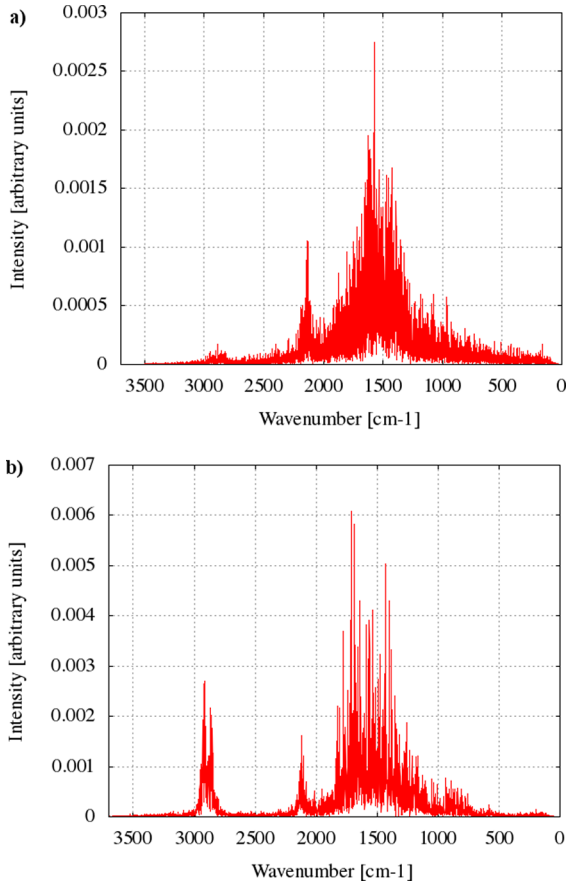

Figure 6. Simulated IR spectra (a) for 3-cyano-2,4-pentanedione and (b) for 4-cyano-2,2,6,6-tetramethyl-3,5-heptanedione.

stretching modes) frequencies from static calculations of crystals and available experimental data together with tentative assignments, are presented in Tables 3 and 4 for crystals **I** and **II**, respectively. Unfortunately, in the experimental IR frequencies, there is a lack of a frequency for the O−H stretching mode.[34] Figures 6 and 7 present the CPMD infrared spectrum for both examined crystals. The calculated spectra show good agreement with experimental results. However, it seems that the CP molecular dynamics method reproduces frequencies of vibrations better than static methods in harmonic approximation in comparison to the experiment. It was observed (see Tables 3 and 4) that the O−H stretching vibrations were quite low in scope of the frequency, about 2151/1823 cm^{-1} and 2150 cm^{-1} for crystal **I** and about 2140/1825 cm^{-1} and 2100 cm^{-1} for crystal **II** in both calculation methods. For example, in the isolated molecules in the gas phase, the static calculated anharmonic frequency for this mode is located at a quite low frequency of about 1738 cm^{-1} and 1729 cm^{-1}, respectively. Calculations for isolated molecules were performed using the Gaussian 09 version c01[52] package on the DFT method level (PBE1PBE/6-311++G(2d,2p)). We would not expect a perfect agreement between the two approaches. There are at least two reasons for noted discrepancies in both calculations. For example, two slightly different density functionals and basis sets were used in both calculations. Moreover, in one of the calculations, we have a perfectly isolated molecule (gas phase), and on the other hand, the molecular system is a crystal environment.

dx.doi.org/10.1021/ct300589r | J. Chem. Theory Comput. 2013, 9, 65−72

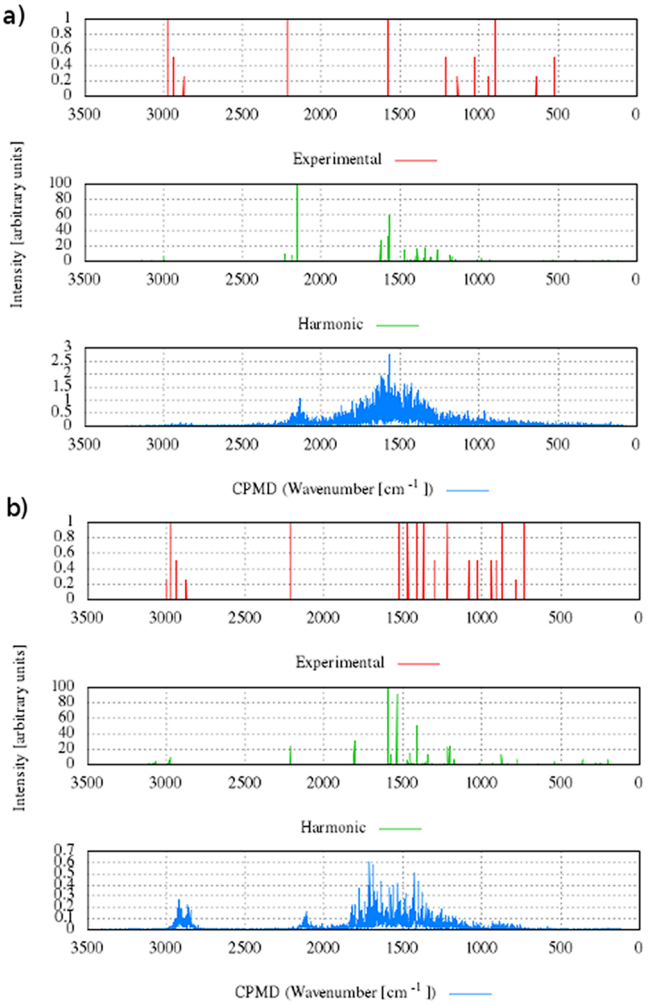

Figure 7. Comparison of the experimental and simulated IR spectra (a) for 3-cyano-2,4-pentanedione and (b) for 4-cyano-2,2,6,6-tetramethyl-3,5-heptanedione.

4. CONCLUSION

In this paper, we have presented the results of theoretical studies on the intramolecular hydrogen bonds in 3-cyano-2,4-pentanedione and 4-cyano-2,2,6,6-tetramethyl-3,5-heptanedione in the solid state. The presented results of both simulations at the CPMD and PIMD levels indicate a large degree of mobility of the proton in the very short O2−HX···O1 intramolecular hydrogen bond. CPMD and CRYSTAL calculations show a good agreement of the optimized geometry with the previously published neutron diffraction study of both crystals.[34,35] The free energy profile and ratio parameter of the proton position suggest that the influences of the crystal structure caused a slight disturbance of the symmetry of the hydrogen bond in spite of the existing keto−enol and enol−keto tautomeric equilibrium. The prevalence of the β-keto−enol form has little to do with the crystal structure. As we expected, it is a consequence of bond energies and steric effects, and the diketo form of these two β-keto−enols would not be found in the gas phase or in solution. The Car−Parrinello molecular dynamics method proved to reproduce the infrared spectra of studied crystals very well, which is in good agreement with the experimental data.

AUTHOR INFORMATION

Corresponding Author

*E-mail: piotr@elrond.chem.uni.wroc.pl. Website: http://kwanty.wchuwr.pl/?q=durlak.

Notes

The authors declare no competing financial interest.

ACKNOWLEDGMENTS

The authors would like to gratefully acknowledge the Ministry of Science and Higher Education of Poland for supporting this research with grant no. 105/10/E-344/M/2011. Thanks are also due to the Academic Computer Centre in Gdansk (CI TASK) for allowing us to use the Galera−ACTION cluster and to the Wroclaw Centre for Networking and Supercomputing (WCSS) for permitting us to use the Supernova Cluster.

REFERENCES

(1) Fillaux, F.; Cousson, A.; Archilla, J. F. R.; Tomkinson, J. *J. Chem. Phys.* **2008**, *128*, 204502−204512.
(2) Morrison, C. A.; Siddick, M. M.; Camp, P. J.; Wilson, C. C. *J. Am. Chem. Soc.* **2005**, *127*, 4042−4048.
(3) Jezierska, A.; Panek, J. J.; Koll, A. *Chem. Phys. Chem.* **2008**, *9*, 839−846.
(4) Jezierska-Mazzarello, A.; Vuilleumier, R.; Panek, J. J.; Ciccotti, G. *J. Phys. Chem. B* **2010**, *114*, 242−253.
(5) Heyne, K; Huse, N.; Dreyer, J.; Nibbering, E. T. J.; Elsa, T. *J. Chem. Phys.* **2004**, *121*, 902−913.
(6) Marx, D.; Tuckerman, M. E.; Hutter, J.; Parrinello, M. *Nature* **1999**, *397*, 601−604.
(7) Tuckerman, M. E.; Marx, D.; Parrinello, M. *Nature* **2002**, *417*, 925−929.
(8) Pirc, G.; Stare, J.; Mavri, J. *J. Chem. Phys.* **2010**, *132*, 224506−224512.
(9) Dopieralski, P. D.; Latajka, Z.; Olovsson, I. *J. Chem. Theory Comput.* **2010**, *6*, 1455−1461.
(10) Cleland, W. W.; Kreevoy, M. M. *Science* **1994**, *264*, 1887−1890.
(11) Berendsen, H.; Mavri, J. Simulating Proton Transfer Processes: Quantum Dynamics Embedded in a Classical Environment. In *Theoretical Treatments of Hydrogen Bonding*, Hadži, D., Ed.; Wiley: New York, 1997; Vol. *8*, pp 119−141.
(12) Gilli, G.; Bellucci, F.; Ferretti, V.; Bertolasi, V. *J. Am. Chem. Soc.* **1989**, *111*, 1023−1028.
(13) Bertolasi, V.; Gilli, P.; Ferretti, V.; Gilli, G. *J. Am. Chem. Soc.* **1991**, *113*, 4917−4925.
(14) Gilli, P.; Bertolasi, V.; Ferretti, V.; Gilli, G. *J. Am. Chem. Soc.* **1994**, *116*, 909−915.
(15) Gilli, P.; Bertolasi, V.; Pretto, L.; Ferretti, V.; Gilli, G. *J. Am. Chem. Soc.* **2004**, *126*, 3845−3855.
(16) Gilli, P.; Bertolasi, V.; Pretto, L.; Antonov, L.; Gilli, G. *J. Am. Chem. Soc.* **2005**, *127*, 4943−4953.
(17) Gilli, G.; Gilli, P. *The Nature of the Hydrogen Bond: Outline of a Comprehensive Hydrogen Bond Theory (International Union of Crystallography Monographs on Crystallography; no. 23)*; Oxford University Press: New York, 2009.
(18) Grabowski, S. J. *J. Phys. Org. Chem.* **2004**, *17*, 18−31.
(19) Sobczyk, L; Grabowski, S. J.; Krygowski, T. M. *Chem. Rev.* **2005**, *105*, 3513−3560.
(20) Lyssenko, K. A.; Antipin, M. Yu. *Russ. Chem. Bull. Int. Ed.* **2006**, *55*, 1−15.
(21) Grabowski, S. J.; Leszczynski, J. In *Hydrogen Bonding-New Insights*; Grabowski, S. J., Ed.; Springer: Berlin, 2006; pp 487−512.
(22) Bertolasi, V.; Ferretti, V.; Gilli, P.; Yao, X.; Li, Ch. -J. *New J. Chem.* **2008**, *32*, 694−704.
(23) Madsen, G. K. H.; Wilson, C.; Nymand, T. M.; McIntyre, G. J.; Larsen, F. K. *J. Phys. Chem. A* **1999**, *103*, 8684−8690.
(24) Hargis, J. C.; Evangelista, F. A.; Ingels, J. B.; Schaefer, H. F., III. *J. Am. Chem. Soc.* **2008**, *130*, 17471−17478.

(25) Hansen, P. E. *Magn. Reson. Chem.* **2008**, *46*, 726−729.
(26) Simonsen, O.; Thorup, N. *Acta Crystallogr., Sect. B* **1979**, *35*, 432−435.
(27) Buemi, G.; Zuccarello, F. *J. Mol. Struct.: THEOCHEM* **2005**, *719*, 137−148.
(28) Sørensen, J.; Clausen, H. F.; Poulsen, R. D.; Overgaard, J.; Schiøtt, B. *J. Phys. Chem. A* **2007**, *111*, 345−351.
(29) Müller, G.; Lutz, M.; Lachmann, J. *Acta Crystallogr., Sect. C* **1994**, *50*, 1318−1320.
(30) Hansen, P. E.; Kamounah, F. S.; Hansen, B. K.; Spanget-Larsen, J. *J. Magn. Reson. Chem.* **2007**, *45*, 106−17.
(31) Durlak, P.; Latajka, Z. *Chem. Phys. Lett.* **2010**, *499*, 56−61.
(32) Belova, N. V.; Girichev, G. V.; Oberhammer, H.; Hoang, T. N.; Shlykov, S. A. *J. Phys. Chem. A* **2012**, *116*, 3428−3435.
(33) Madsen, G. K.; McIntyre, G. J.; Schiøtt, B.; Larsen, F. K. *Chem.—Eur. J.* **2007**, *13*, 5539−5547.
(34) Silvernail, C. M.; Yap, G.; Sommer, R. D.; Rheingold, A. L.; Day, V. W.; Belot, J. A. *Polyhedron* **2001**, *20*, 3113−3117.
(35) Belot, J. A.; Clark, J.; Cowan, J. A.; Harbison, G. S.; Kolesnikov, A. I.; Kye, Y. -S.; Schultz, A. J.; Silvernail, C.; Zhao, X. *J. Phys. Chem.* **2004**, *B108*, 6922−6926.
(36) Marx, D. Advanced Car-Parrinello Techniques: Path Integrals and Nonadiabaticity In Condensed Matter Simulations. In *Computer Simulations in Condensed Matter Systems: From Materials to Chemical Biology Vol. 2, Lect. Notes Phys.*; Ferrario, M., Ciccotti, G., Binder, K., Eds.; Springer: Berlin, 2006; Vol. *704*, pp 507−539.
(37) Tuckerman, M. E. Path Integration via Molecular Dynamics. In *Quantum Simulation of Complex Many-Body Systems: From Theory to Algorithms*; Grotendorst, J., Marx, D., Muramatsu, A., Eds.; John von Neumann Instituite for Computing (NIC): Juelich, Germany, 2002; Vol. *10*, pp 269−298.
(38) Grimme, S. *J. Comput. Chem.* **2006**, *27*, 1787−1799.
(39) Dovesi, R.; Saunders, V. R.; Roetti, C.; Orlando, R.; Zicovich-Wilson, C. M.; Pascale, F.; Civalleri, B.; Doll, K.; Harrison, N. M.; Bush, I. J.; D'Arco, Ph.; Llunell, M. *CRYSTAL09 User's Manual*, University of Torino: Torino, Italy, 2009.
(40) Dovesi, R.; Orlando, R.; Civalleri, B.; Roetti, C.; Saunders, V. R.; Zicovich-Wilson, C. M. *Z. Kristallogr.* **2005**, *220*, 571−573.
(41) Perdew, J. P.; Burke, K.; Ernzerhof, M. *Phys. Rev. Lett.* **1996**, *77*, 3865−3868.
(42) Monkhorst, H. J.; Pack, J. D. *Phys. Rev.* **1976**, *B13*, 5188−5192.
(43) Gatti, C.; Saunders, V. R.; Roetti, C. *J. Chem. Phys.* **1994**, *101*, 10686−10696.
(44) *CPMD*, version 3.13.2; IBM Corp.: Armonk, NY, 1990−2008, MPI für Festkörperforschung Stuttgart: Stuttgart, Germany, 1997−2001. http://www.cpmd.org (accessed October 2012).
(45) Martyna, G. J.; Klein, M. L.; Tuckerman, M. *J. Chem. Phys.* **1992**, *97*, 2635−2643.
(46) Troullier, N.; Martins, J. L. *Phys. Rev.* **1991**, *B43*, 1993−2006.
(47) Humphrey, W.; Dalke, A.; Schulten, K. *J. Mol. Graphics* **1996**, *14*, 33−38.
(48) Kohlmeyer, A.; Forbert, H. *traj2xyz.pl*, version 1.4.; 2004.
(49) Forbert, H.; Kohlmeyer, A. *Fourier*, version 2; 2002−05.
(50) Wilson, C. C.; Shankland, N.; Florence, A. J. *Chem. Phys. Lett.* **1996**, *253*, 103−107.
(51) Durlak, P.; Latajka, Z. *Chem. Phys. Lett.* **2009**, *447*, 249−254.
(52) Frisch, M. J.; Trucks, G. W.; Schlegel, H. B.; Scuseria, G. E.; Robb, M. A.; Cheeseman, J. R.; Scalmani, G.; Barone, V.; Mennucci, B.; Petersson, G. A.; Nakatsuji, H.; Caricato, M.; Li, X.; Hratchian, H. P.; Izmaylov, A. F.; Bloino, J.; Zheng, G.; Sonnenberg, J. L.; Hada, M.; Ehara, M.; Toyota, K.; Fukuda, R.; Hasegawa, J.; Ishida, M.; Nakajima, T.; Honda, Y.; Kitao, O.; Nakai, H.; Vreven, T.; Montgomery, J. A., Jr.; Peralta, J. E.; Ogliaro, F.; Bearpark, M.; Heyd, J. J.; Brothers, E.; Kudin, K. N.; Staroverov, V. N.; Kobayashi, R.; Normand, J.; Raghavachari, K.; Rendell, A.; Burant, J. C.; Iyengar, S. S.; Tomasi, J.; Cossi, M.; Rega, N.; Millam, J. M.; Klene, M.; Knox, J. E.; Cross, J. B.; Bakken, V.; Adamo, C.; Jaramillo, J.; Gomperts, R.; Stratmann, R. E.; Yazyev, O.; Austin, A. J.; Cammi, R.; Pomelli, C.; Ochterski, J. W.; Martin, R. L.; Morokuma, K.; Zakrzewski, V. G.; Voth, G. A.; Salvador, P.; Dannenberg, J. J.; Dapprich, S.; Daniels, A. D.; Farkas, Ö.; Foresman, J. B.; Ortiz, J. V.; Cioslowski, J.; Fox, D. J. *Gaussian 09*, revision C.01; Gaussian, Inc.: Wallingford CT, 2009.